

Calculation of renormalized viscosity and resistivity in magnetohydrodynamic turbulence

Mahendra K. Verma ^{*}

Department of Physics, Indian Institute of Technology, Kanpur – 208016, INDIA

(February 5, 2020)

A self-consistent renormalization (RG) scheme has been applied to nonhelical magnetohydrodynamic turbulence with zero cross helicity. Kolmogorov's 5/3 powerlaw has been shown to be a consistent solution of RG equations for space-dimensions $d \geq d_c \approx 2.2$. The RG fixed point is unstable for $d = 2$. The renormalized viscosity ν^* and resistivity λ^* have been calculated, and they are found to be positive for all parameter regimes. For large d , both ν^* and λ^* vary as $d^{-1/2}$ for a fixed r_A . The variation of the renormalized parameters with r_A at $d = 3$ has also been studied.

PACS numbers: 47.27.Gs, 52.35.Ra, 11.10.Gh

I. INTRODUCTION

The Renormalization Group (RG) technique provided an important tool for understanding of phase transitions and critical phenomena. Motivated by this success, researchers have applied this technique to turbulence and other nonequilibrium systems. In this paper we apply RG to magnetohydrodynamic (MHD) turbulence.

Forster et al. [1] first applied dynamical RG procedure to the analysis of Navier-Stokes and Burgers equations, both stirred by random forces. They eliminated the large-wavenumber modes and included the effects of nonlinearity in the effective viscosity. Later, DeDominicis and Martin [2], Fournier and Frisch [3], Yakhot and Orszag [4], many others studied various aspects of RG for fluid turbulence, but all of them considered certain form of external forcing. McComb and his coworkers ([5,6] and reference therein) instead applied self-consistent RG procedure; here the energy spectrum was assumed to be Kolmogorov's spectrum, and the renormalized viscosity was computed iteratively. We have adopted a similar scheme for MHD turbulence.

Fournier et al. [7], Camargo and Tasso [8], and Liang and Diamond [9] employed RG technique to MHD turbulence on the similar lines as adopted by Forster et al. [1] for fluid turbulence. Fournier et al. [7] found that for $d > d_c \approx 2.8$, there are two nontrivial regimes: a kinetic regime where the renormalization of the transport coefficients is due to kinetic small-scales; and a magnetic regime where it is due to the magnetic small-scales. In dimensions $2 \leq d \leq d_c$, there is no stable fixed point for turbulence with sufficiently strong external currents. Camargo and Tasso [8] studied the effective (renormalized) viscosity and resistivity and concluded that negative viscosity and resistivity are not permissible except in certain cases. Liang and Diamond [9] showed that no RG fixed point exists in 2D MHD turbulence. All the above authors however do not give any clear idea about the energy spectrum of MHD turbulence, which still remains controversial.

Kraichnan [11] and Iroshnikov [12] first gave phenomenology of steady-state, homogeneous, and isotropic MHD turbulence. They argued that the kinetic and magnetic energy spectra ($E^u(k)$ and $E^b(k)$ respectively) are

$$E^u(k) = E^b(k) = A(\Pi B_0)^{1/2} k^{-3/2} \quad (1.1)$$

where Π is the total energy cascade rate, B_0 is the mean magnetic field or the magnetic field of the largest eddy, and A is universal constant of order one. Later Marsch [13], Matthaeus and Zhou [14], and Zhou and Matthaeus [15] proposed an alternate phenomenology in which the energy spectra $E^\pm(k)$ of Elsässer variables $\mathbf{z}^\pm (= \mathbf{u} \pm \mathbf{b})$ are

$$E^\pm(k) = K^\pm \frac{(\Pi^\pm)^{4/3}}{(\Pi^\mp)^{2/3}} k^{-5/3} \quad (1.2)$$

^{*}email: mkv@iitk.ac.in

where Π^\pm are the energy cascade rates of z^\pm , and K^\pm are the Kolmogorov's constants for MHD.

The energy spectrum of the solar wind, a well known observational platform for MHD turbulence, is closer to $k^{-5/3}$ than to $k^{-3/2}$ [16,17]. In addition, the recent numerical [18–20] and theoretical [10,21,22] work support Kolmogorov-like phenomenology for MHD turbulence. Verma [10] showed that the mean magnetic field B_0 appearing in Kraichnan's formula (1.1) gets renormalized ($B_0(k) \propto k^{-1/3}$) in strong turbulence. When we substitute the renormalized B_0 in Eq. (1.1), the energy spectrum turns out to be proportional to $k^{-5/3}$. Sridhar and Goldreich, and Goldreich and Sridhar [21,22] used wave interaction picture and showed that the energy spectrum is anisotropic, and it follows Kolmogorov's powerlaw for strong turbulence.

In this paper we calculate the renormalized viscosity and resistivity for MHD. Here we test whether Kolmogorov's spectrum is a consistent solution of RG or not if the turbulence is forced at large-scale. We carry out wavenumber elimination and obtain a recursive RG equation. The Kolmogorov's spectrum is substituted for the correlation function in the recursive RG equation. After that we attempt to obtain a convergent solution for the renormalized viscosity and resistivity. If the convergent solution exists, then the Kolmogorov's spectrum is one of the correct choices for the energy spectrum of MHD turbulence. For this cases we have computed many important quantities, e.g., renormalized viscosity, renormalized resistivity, cascade rates etc., in a reasonably simple manner. In this paper we report the calculation of renormalized viscosity and resistivity, and in the subsequent paper (referred to as paper II) we report the cascade rate calculation.

There are two field variables in MHD: the velocity fluctuation \mathbf{u} and the magnetic field fluctuation \mathbf{b} . The quantities of interest are Kinetic energy (KE), magnetic energy (ME), total energy (KE+ME), and cross helicity ($H_c = \mathbf{u} \cdot \mathbf{b}$). The dimensionless parameters used in this paper are the ratio of twice the cross helicity and the total energy, called normalized cross helicity σ_c ($\sigma_c = 2H_c/(KE + ME)$), and the ratio of KE and ME, called Alfvén ratio r_A . In this paper we have assumed that the mean magnetic field is zero, and so are magnetic and kinetic helicities, i.e., we are considering nonhelical plasma. Calculation of the renormalized parameters is quite complex for arbitrary σ_c and r_A . Therefore, we limit ourselves to two limiting cases (1) $\sigma_c = 0$ and whole range of r_A ; (2) $\sigma_c \rightarrow 1$ and $r_A = 1$. Even though full range of σ_c is observed in terrestrial and extraterrestrial plasmas, the $\sigma_c \approx 0$ case is most pronounced.

The outline of the paper is as follows: in sections 2 and 3 we compute the renormalized viscosity and resistivity for $\sigma_c = 0$ and $\sigma_c \rightarrow 1$ cases respectively. Section 4 contains the summary and conclusions.

II. RG CALCULATION: $\sigma_c = 0$

In this section we will calculate the renormalized viscosity and resistivity of MHD equations for zero mean magnetic field and zero cross helicity ($\sigma_c = 0$). In this case, the RG equations in terms of velocity and magnetic field variables are simpler as compared to Elsässer variables. Therefore, we will work with \mathbf{u} and \mathbf{b} variables. We take the following form of Kolmogorov's spectrum for KE [$E^u(k)$] and ME [$E^b(k)$]

$$E^u(k) = K^u \Pi^{2/3} k^{-5/3} \quad (2.1)$$

$$E^b(k) = E^u(k)/r_A \quad (2.2)$$

where K^u is Kolmogorov's constant for MHD turbulence, and Π is the total energy flux. In the limit $\sigma_c = 0$, we have $E^+ = E^-$ and $\Pi^+ = \Pi^- = \Pi$ [cf. Eq. (1.2)]. Therefore, $E_{total}(k) = E^+(K) = E^u(k) + E^b(k)$ and

$$K^+ = K^u(1 + r_A^{-1}) \quad (2.3)$$

With this preliminaries we start our RG calculation. The incompressible MHD equation in the Fourier space is

$$(-i\omega + \nu k^2) u_i(\hat{k}) = -\frac{i}{2} P_{ijm}^+(\mathbf{k}) \int d\hat{p} [u_j(\hat{p}) u_m(\hat{k} - \hat{p}) - b_j(\hat{p}) b_m(\hat{k} - \hat{p})] \quad (2.4)$$

$$(-i\omega + \lambda k^2) b_i(\hat{k}) = -i P_{ijm}^-(\mathbf{k}) \int d\hat{p} [u_j(\hat{p}) b_m(\hat{k} - \hat{p})] \quad (2.5)$$

$$k_i u_i(\mathbf{k}) = 0 \quad (2.6)$$

$$k_i b_i(\mathbf{k}) = 0 \quad (2.7)$$

with

$$P_{ijm}^+(\mathbf{k}) = k_j P_{im}(\mathbf{k}) + k_m P_{ij}(\mathbf{k}); \quad (2.8)$$

$$P_{im}(\mathbf{k}) = \delta_{im} - \frac{k_i k_m}{k^2}; \quad (2.9)$$

$$P_{ijm}^-(\mathbf{k}) = k_j \delta_{im} - k_m \delta_{ij}; \quad (2.10)$$

$$\hat{k} = (\mathbf{k}, \omega); \quad (2.11)$$

$$d\hat{p} = d\mathbf{p}d\omega/(2\pi)^{d+1}. \quad (2.12)$$

Here ν and λ are the viscosity and the resistivity respectively, and d is the space dimension.

In our RG procedure the wavenumber range (k_N, k_0) is divided logarithmically into N shells. The n th shell is (k_n, k_{n-1}) where $k_n = h^n k_0$ ($h < 1$). In the following discussion, we carry out the elimination of the first shell (k_1, k_0) and obtain the modified MHD equation. We then proceed iteratively to eliminate higher shells and get a general expression for the modified MHD equation. The details of the renormalization group calculation is as follows:

1. We divide the spectral space into two parts: 1. the shell $(k_1, k_0) = k^>$, which is to be eliminated; 2. $(k_N, k_1) = k^<$, set of modes to be retained. Note that ν_0 and λ_0 denote the viscosity and resistivity before the elimination of the first shell.
2. We rewrite the Eqs. (2.4, 2.5) for $k^<$ and $k^>$. The equation for $u_i^<(\hat{k})$ and $b_i^<(\hat{k})$ modes are

$$\begin{aligned} \left(-i\omega + \Sigma_{(0)}^{uu}(k) \right) u_i^<(\hat{k}) + \Sigma_{(0)}^{ub}(k) b_i^<(\hat{k}) &= -\frac{i}{2} P_{ijm}^+(\mathbf{k}) \int d\hat{p} ([u_j^<(\hat{p}) u_m^<(\hat{k} - \hat{p})] \\ &\quad + [u_j^<(\hat{p}) u_m^>(\hat{k} - \hat{p})] + [u_j^>(\hat{p}) u_m^>(\hat{k} - \hat{p})] \\ &\quad - \text{Similar terms for } b) \end{aligned} \quad (2.13)$$

$$\begin{aligned} \left(-i\omega + \Sigma_{(0)}^{bb}(k) \right) b_i^<(\hat{k}) + \Sigma_{(0)}^{bu}(k) u_i^<(\hat{k}) &= -i P_{ijm}^-(\mathbf{k}) \int d\hat{p} ([u_j^<(\hat{p}) b_m^<(\hat{k} - \hat{p})] \\ &\quad + [u_j^<(\hat{p}) b_m^>(\hat{k} - \hat{p})] + [u_j^>(\hat{p}) b_m^>(\hat{k} - \hat{p})] \\ &\quad + [u_j^>(\hat{p}) b_m^>(\hat{k} - \hat{p})]) \end{aligned} \quad (2.14)$$

Σ s appearing in the equations are usually called self-energy in Quantum field theory language. In the first iteration, $\Sigma_{(0)}^{uu} = \nu_{(0)} k^2$ and $\Sigma_{(0)}^{bb} = \lambda_{(0)} k^2$, while the other two Σ s are zero. The equation for $u_i^>(\hat{k})$ modes can be obtained by interchanging $<$ and $>$ in the above equations.

3. The terms given in the second and third brackets in the RHS of Eqs. (2.13, 2.14) are calculated perturbatively. Since we are interested in the statistical properties of \mathbf{u} and \mathbf{b} fluctuations, we perform the usual ensemble average of the system [4]. We assume that $\mathbf{u}^>(\hat{k})$ and $\mathbf{b}^>(\hat{k})$ have gaussian distributions with zero mean, while $\mathbf{u}^<(\hat{k})$ and $\mathbf{b}^<(\hat{k})$ are unaffected by the averaging process. Hence,

$$\langle u_i^>(\hat{k}) \rangle = 0 \quad (2.15)$$

$$\langle b_i^>(\hat{k}) \rangle = 0 \quad (2.16)$$

$$\langle u_i^<(\hat{k}) \rangle = u_i^<(\hat{k}) \quad (2.17)$$

$$\langle b_i^<(\hat{k}) \rangle = b_i^<(\hat{k}) \quad (2.18)$$

and

$$\langle u_i^>(\hat{p}) u_j^>(\hat{q}) \rangle = P_{ij}(\mathbf{p}) C^{uu}(\hat{p}) \delta(\hat{p} + \hat{q}) \quad (2.19)$$

$$\langle b_i^>(\hat{p}) b_j^>(\hat{q}) \rangle = P_{ij}(\mathbf{p}) C^{bb}(\hat{p}) \delta(\hat{p} + \hat{q}) \quad (2.20)$$

$$\langle u_i^>(\hat{p}) b_j^>(\hat{q}) \rangle = P_{ij}(\mathbf{p}) C^{ub}(\hat{p}) \delta(\hat{p} + \hat{q}) \quad (2.21)$$

The triple order correlations $\langle X_i^>(\hat{k}) X_j^>(\hat{p}) X_m^>(\hat{q}) \rangle$ are zero due to Gaussian nature of the fluctuations. Here, X stands for u or b . In addition, we also neglect the contribution from the triple nonlinearity $\langle X_i^<(\hat{k}) X_j^<(\hat{p}) X_m^<(\hat{q}) \rangle$. The last assumption is used in many the turbulence RG calculations [4,5]. Refer to Zhou and Vahala [25] for discussion on inclusion of triple nonlinearity.

4. The details of the calculation is given in Appendix A. To the first order, the second bracketed terms of Eqs. (2.13, 2.14) vanish, but the third bracketed terms are nonzero. These quantities yield correction to Σ s. The Eqs. (2.13, 2.14) now become

$$\left(-i\omega + \Sigma_{(0)}^{uu} + \delta\Sigma_{(0)}^{uu}\right) u_i^<(\hat{k}) + \left(\Sigma_{(0)}^{ub} + \delta\Sigma_{(0)}^{ub}\right) b_i^<(\hat{k}) = -\frac{i}{2} P_{ijm}^+(\mathbf{k}) \int d\hat{p} [u_j^<(\hat{p}) u_m^<(\hat{k} - \hat{p}) - b_j^<(\hat{p}) b_m^<(\hat{k} - \hat{p})] \quad (2.22)$$

$$\left(-i\omega + \Sigma_{(0)}^{bb} + \delta\Sigma_{(0)}^{bb}\right) b_i^<(\hat{k}) + \left(\Sigma_{(0)}^{bu} + \delta\Sigma_{(0)}^{bu}\right) u_i^<(\hat{k}) = -i P_{ijm}^-(\mathbf{k}) \int d\hat{p} [u_j^<(\hat{p}) b_m^<(\hat{k} - \hat{p})] \quad (2.23)$$

with

$$\begin{aligned} \delta\Sigma_{(0)}^{uu}(k) &= \frac{1}{(d-1)k^2} \int_{\hat{p}+\hat{q}=\hat{k}}^{\Delta} d\hat{p} [S(k, p, q) G^{uu}(\hat{p}) C^{uu}(\hat{q}) - S_6(k, p, q) G^{bb}(\hat{p}) C^{bb}(\hat{q}) \\ &\quad + S_6(k, p, q) G^{ub}(\hat{p}) C^{ub}(\hat{q}) - S(k, p, q) G^{bu}(\hat{p}) C^{ub}(\hat{q})] \end{aligned} \quad (2.24)$$

$$\begin{aligned} \delta\Sigma_{(0)}^{ub}(k) &= \frac{1}{(d-1)k^2} \int_{\hat{p}+\hat{q}=\hat{k}}^{\Delta} d\hat{p} [-S(k, p, q) G^{uu}(\hat{p}) C^{ub}(\hat{q}) + S_5(k, p, q) G^{ub}(\hat{p}) C^{uu}(\hat{q}) \\ &\quad + S(k, p, q) G^{bu}(\hat{p}) C^{bb}(\hat{q}) - S_5(k, p, q) G^{bb}(\hat{p}) C^{ub}(\hat{q})] \end{aligned} \quad (2.25)$$

$$\begin{aligned} \delta\Sigma_{(0)}^{bu}(k) &= \frac{1}{(d-1)k^2} \int_{\hat{p}+\hat{q}=\hat{k}}^{\Delta} d\hat{p} [S_8(k, p, q) G^{uu}(\hat{p}) C^{ub}(\hat{q}) + S_{10}(k, p, q) G^{bb}(\hat{p}) C^{ub}(\hat{q}) \\ &\quad + S_{12}(k, p, q) G^{ub}(\hat{p}) C^{bb}(\hat{q}) - S_7(k, p, q) G^{bu}(\hat{p}) C^{uu}(\hat{q})] \end{aligned} \quad (2.26)$$

$$\begin{aligned} \delta\Sigma_{(0)}^{bb}(k) &= \frac{1}{(d-1)k^2} \int_{\hat{p}+\hat{q}=\hat{k}}^{\Delta} d\hat{p} [-S_8(k, p, q) G^{uu}(\hat{p}) C^{bb}(\hat{q}) + S_9(k, p, q) G^{bb}(\hat{p}) C^{uu}(\hat{q}) \\ &\quad + S_{11}(k, p, q) G^{ub}(\hat{p}) C^{ub}(\hat{q}) - S_9(k, p, q) G^{bu}(\hat{p}) C^{ub}(\hat{q})] \end{aligned} \quad (2.27)$$

The quantities $S_i(k, p, q)$ are given in the Appendix B. The integral Δ is to be done over the first shell.

The full-fledge calculation of Σ s is quite involved. Therefore, we take two special cases: (1) $C^{ub} = 0$ or $\sigma_c = 0$; and (2) $C^{ub} \approx C^{uu} \approx C^{ub}$ or $\sigma_c \rightarrow 1$. In this section we will discuss only $\sigma_c = 0$ case. The other case will be taken up in the next section.

When $\sigma_c = 0$, an inspection of the self-energy diagrams shows that $\Sigma^{ub} = \Sigma^{bu} = 0$, and $G^{ub} = G^{bu} = 0$. Clearly, the equations become much simpler because of the diagonal nature of matrices G and Σ . The two quantities of interest $\delta\Sigma_{(0)}^{uu}$ and $\delta\Sigma_{(0)}^{bb}$ will be given by

$$\delta\Sigma_{(0)}^{uu}(\hat{k}) = \frac{1}{d-1} \int_{\hat{p}+\hat{q}=\hat{k}}^{\Delta} d\hat{p} (S(k, p, q) G^{uu}(p) C^{uu}(q) - S_6(k, p, q) G^{bb}(p) C^{bb}(q)) \quad (2.28)$$

$$\delta\Sigma_{(0)}^{bb}(\hat{k}) = \frac{1}{d-1} \int_{\hat{p}+\hat{q}=\hat{k}}^{\Delta} d\hat{p} (-S_8(k, p, q) G^{uu}(p) C^{bb}(q) + S_9(k, p, q) G^{bb}(p) C^{uu}(q)) \quad (2.29)$$

The expressions for $\delta\Sigma$'s involves correlation functions and Green's function, which are themselves functions of Σ 's. In earlier RG calculations (see e.g. [1,4]) the correlation function $C(\hat{k})$ is function of forcing noise spectrum. In our self-consistent scheme we assume that we are in inertial range, and the energy spectrum is proportional to Kolmogorov's 5/3 powerlaw. After that the renormalized Green's function, or renormalized ν is computed iteratively.

The frequency dependence of the correlation function are taken as: $C^{uu}(k, \omega) = 2C^{uu}(k)\Re(G^{uu}(k, \omega))$ and $C^{bb}(k, \omega) = 2C^{bb}(k)\Re(G^{bb}(k, \omega))$. In other words, the relaxation time-scale of correlation function is assumed to be the same as that of corresponding Greens function. Since we are interested in large time-scale behaviour of turbulence, we take the limit ω going to zero. Under these assumptions, the above equations become

$$\delta\nu_{(0)}(k) = \frac{1}{(d-1)k^2} \int_{\hat{p}+\hat{q}=\hat{k}}^{\Delta} \frac{d\mathbf{p}}{(2\pi)^d} [S(k, p, q) \frac{C^{uu}(q)}{\nu_{(0)}(p)p^2 + \nu_{(0)}(q)q^2}$$

$$-S_6(k, p, q) \frac{C^{bb}(q)}{\lambda_{(0)}(p)p^2 + \lambda_{(0)}(q)q^2}] \quad (2.30)$$

$$\begin{aligned} \delta\lambda_{(0)}(k) = \frac{1}{(d-1)k^2} \int_{\hat{p}+\hat{q}=\hat{k}}^{\Delta} \frac{d\mathbf{p}}{(2\pi)^d} & [-S_9(k, p, q) \frac{C^{bb}(q)}{\nu_{(0)}(p)p^2 + \lambda_{(0)}(q)q^2} \\ & + S_9(k, p, q) \frac{C^{uu}(q)}{\lambda_{(0)}(p)p^2 + \nu_{(0)}(q)q^2}] \end{aligned} \quad (2.31)$$

Note that $\nu(k) = \Sigma^{uu}(k)/k^2$ and $\lambda(k) = \Sigma^{bb}(k)/k^2$.

There are some important points to remember in the above step. The frequency integral in the above is done using contour integral. It can be shown that the integrals are nonzero only when both the components appearing the denominator are of the same sign. For example, first term of Eq. (2.31) is nonzero only when both $\nu_{(0)}(p)$ and $\lambda_{(0)}(q)$ are of the same sign.

Let us denote $\nu_{(1)}(k)$ and $\lambda_{(1)}(k)$ as the renormalized viscosity and resistivity respectively after the first step of wavenumber elimination. Hence,

$$\nu_{(1)}(k) = \nu_{(0)}(k) + \delta\nu_{(0)}(k); \quad (2.32)$$

$$\lambda_{(1)}(k) = \lambda_{(0)}(k) + \delta\lambda_{(0)}(k) \quad (2.33)$$

5. We keep eliminating the shells one after the other by the above procedure. After $n+1$ iterations we obtain

$$\nu_{(n+1)}(k) = \nu_{(n)}(k) + \delta\nu_{(n)}(k) \quad (2.34)$$

$$\lambda_{(n+1)}(k) = \lambda_{(n)}(k) + \delta\lambda_{(n)}(k) \quad (2.35)$$

where the equations for $\delta\nu_{(n)}(k)$ s are the same as the Eqs. (2.30, 2.31) except that $\nu_{(0)}(k)$ and $\lambda_{(0)}(k)$ appearing in the equations are to be replaced by $\nu_{(n)}(k)$ and $\lambda_{(n)}(k)$ respectively. Clearly $\nu_{(n+1)}(k)$ and $\lambda_{(n+1)}(k)$ are the renormalized viscosity and resistivity after the elimination of the $(n+1)$ th shell.

6. We need to compute $\delta\nu_{(n+1)}$ and $\delta\lambda_{(n+1)}$ for various n . These computations, however, require $\nu_{(n)}$ and $\lambda_{(n)}$. In our scheme we solve these equations iteratively. In Eqs. (2.30, 2.31) we substitute $C(k)$ by one dimensional energy spectrum $E(k)$

$$C^{uu}(k) = \frac{2(2\pi)^d}{S_d(d-1)} k^{-(d-1)} E^u(k) \quad (2.36)$$

$$C^{bb}(k) = \frac{2(2\pi)^d}{S_d(d-1)} k^{-(d-1)} E^b(k) \quad (2.37)$$

where S_d is the surface area of d dimensional spheres. We assume that $E^u(k)$ and $E^b(k)$ follow Eqs. (2.1, 2.2) respectively. Regarding $\nu_{(n)}$ and $\lambda_{(n)}$, we attempt the following form of solution

$$\nu_{(n)}(k_n k') = (K^u)^{1/2} \Pi^{1/3} k_n^{-4/3} \nu_{(n)}^*(k') \quad (2.38)$$

$$\lambda_{(n)}(k_n k') = (K^u)^{1/2} \Pi^{1/3} k_n^{-4/3} \lambda_{(n)}^*(k') \quad (2.39)$$

with $k = k_{n+1} k'$ ($k' < 1$). We expect $\nu_{(n)}^*(k')$ and $\lambda_{(n)}^*(k')$ to be universal functions for large n . The substitution of $C^{uu}(k)$, $C^{bb}(k)$, $\nu_{(n)}(k)$, and $\lambda_{(n)}(k)$ yields the following equations for $\nu_{(n+1)}^*(k')$ and $\lambda_{(n+1)}^*(k')$:

$$\begin{aligned} \delta\nu_{(n)}^*(k') = \frac{1}{(d-1)} \int_{\mathbf{p}'+\mathbf{q}'=\mathbf{k}'} d\mathbf{q}' \frac{2}{(d-1)S_d} \frac{E^u(q')}{q'^{d-1}} \times \\ \left[S(k', p', q') \frac{1}{\nu_{(n)}^*(hp')p'^2 + \nu_{(n)}^*(hq')q'^2} - S_6(k', p', q') \frac{r_A^{-1}}{\lambda_{(n)}^*(hp')p'^2 + \lambda_{(n)}^*(hq')q'^2} \right] \end{aligned} \quad (2.40)$$

$$\delta\lambda_{(n)}^*(k') = \frac{1}{(d-1)} \int_{\mathbf{p}'+\mathbf{q}'=\mathbf{k}'} d\mathbf{q}' \frac{2}{(d-1)S_d} \frac{E^u(q')}{q'^{d-1}} \times$$

$$\left[-S_8(k', p', q') \frac{1}{\nu_{(n)}^*(hp')p'^2 + \lambda_{(n)}^*(hq')q'^2} + S_9(k', p', q') \frac{r_A^{-1}}{\lambda_{(n)}^*(hp')p'^2 + \nu_{(n)}^*(hq')q'^2} \right] \quad (2.41)$$

$$\nu_{(n+1)}^*(k') = h^{4/3} \nu_{(n)}^*(hk') + h^{-4/3} \delta \nu_{(n)}^*(k') \quad (2.42)$$

$$\lambda_{(n+1)}^*(k') = h^{4/3} \lambda_{(n)}^*(hk') + h^{-4/3} \delta \lambda_{(n)}^*(hk') \quad (2.43)$$

where the integrals in the above equations are performed iteratively over a region $1 \leq p', q' \leq 1/h$ with the constraint that $\mathbf{p}' + \mathbf{q}' = \mathbf{k}'$. Fournier and Frisch [3] showed the above volume integral in d dimension to be

$$\int_{\mathbf{p}' + \mathbf{q}' = \mathbf{k}'} d\mathbf{q}' = S_{d-1} \int dp dq \left(\frac{pq}{k} \right)^{d-2} (\sin \alpha)^{d-3} \quad (2.44)$$

where α is the angle between vectors \mathbf{p} and \mathbf{q} .

7. Now we solve the above four equations self consistently for various r_A s. We have taken $h = 0.7$. We start with constant values of $\nu_{(0)}^*$ and $\lambda_{(0)}^*$ and compute the integrals using Gauss quadrature technique. Once $\delta \nu_{(0)}$ and $\delta \lambda_{(0)}$ have been computed, we can calculate $\nu_{(1)}^*$ and $\lambda_{(1)}^*$. We iterate this process till $\nu_{(m+1)}^*(k') \approx \nu_{(m)}^*(k')$ and $\lambda_{(m+1)}^*(k') \approx \lambda_{(m)}^*(k')$, that is, till they converge. We have reported the limiting ν^* and λ^* whenever the solution converges. The result of our RG analysis is given below.

We have carried out the RG analysis for various space dimensions and find that the solution converges for all $d > d_c \approx 2.2$. Hence, the RG fixed-point for MHD turbulence is stable for $d \geq d_c$. For illustration of convergent solution, see the plots of $\nu_{(n)}^*(k')$ and $\lambda_{(n)}^*(k')$ for $d = 3, r_A = 1$ in Fig. 1. The RG fixed point for $d < d_c$ is unstable. Refer to the plots of Fig. 2 for $d = 2, r_A = 1$ for an example of unstable solution. From this observation we can claim that Kolmogorov's powerlaw is a consistent solution of MHD RG equations at least for $d \geq d_c$. The values of asymptotic ($k' \rightarrow 0$ limit) ν^* and λ^* for various d and $r_A = 1$ are displayed in Table I. Clearly ν^* and λ^* decreases with the increase in d for $d \geq 4$. The plot of Fig. (3) shows that both ν^* and λ^* are proportional to $d^{-1/2}$. In the same plot we have also displayed ν^* for pure fluid turbulence; there too $\nu^* \propto d^{-1/2}$. This result is consistent with Fournier et al.'s prediction for fluid turbulence [23].

An important point to note is that the stability of RG fixed point in a given space dimension depends on Alfvén ratio and normalized cross helicity. For example, for $d = 2.2$ the RG fixed point is stable for $r_A \geq 1$. A detailed study of stability of the RG fixed point is required to ascertain the boundary of stability.

The values of renormalized parameters for $d = 3$ and various r_A are shown in Table II. For large r_A (fluid dominated regime), ν^* is close to renormalized viscosity of fluid turbulence ($r_A = \infty$), but λ^* is also finite. That means there is a positive magnetic energy flux even when $r_A \rightarrow \infty$. As r_A is decreased, λ^* decreases but ν^* increases. This trend is seen till $r_A \approx 0.25$ where the RG fixed point with nonzero ν^* and λ^* becomes unstable, and the trivial RG fixed point with $\nu^* = \lambda^* = 0$ becomes stable. This result suggests an absence of turbulence for r_A approximately below 0.25. Note that in the $r_A \rightarrow 0$ (fully magnetic) limit, the MHD equations become linear, hence there is no turbulence. Surprisingly, our RG calculation suggests that turbulence disappear near $r_A = 0.25$ itself.

The final $\nu^*(k')$ and $\lambda^*(k')$ are constant for small k' but shifts towards zero for larger k' (see Fig. 1). Similar behaviour has been seen by McComb and coworkers [24] for fluid turbulence; this behaviour is attributed to the neglect of triple nonlinearity, and the corrective procedure has been prescribed by Zhou and Vahala [25]. For simplicity we have not included triple nonlinearity in our calculation.

Pouquet [26] and Ishizawa and Hattori [27] calculated the contributions to renormalized (eddy) viscosity and resistivity from each of the four nonlinear terms of MHD equations using EDQNM approximation for $d = 2$. Let us denote the quantities $\nu^{uu}, \nu^{ub}, \lambda^{bu}, \lambda^{bb}$ as contributions from the terms $\mathbf{u} \cdot \nabla \mathbf{u}, -\mathbf{b} \cdot \nabla \mathbf{b}, -\mathbf{u} \cdot \nabla \mathbf{b}, \mathbf{b} \cdot \nabla \mathbf{u}$ respectively. Note that various cascade rates of MHD turbulence [28,29] can be inferred from these parameters. The cascade rate from inside of the X sphere ($X <$) to outside of the Y sphere ($Y >$) is

$$\Pi_{Y>}^{X<} = \int_0^{k_N} 2\nu^{XY}(k)k^2 E^X(k) dk \quad (2.45)$$

where X, Y denote u or b . We have computed ν^{XY} for $d \geq d_c$; their values are listed in Tables I and II. Our results show that λ^{bb} is positive. Pouquet argues that λ^{bb} is negative, while Ishizawa finds it to be positive. Since our RG procedure is applicable only for $d > d_c = 2.2$, it is not proper to compare our results with those of Pouquet [26] and Ishizawa and Hattori [27]. However, we can claim that the magnetic energy cascade rate ($\Pi_b^{b<}$) is positive for all $d > d_c$ because $\lambda^{bb} > 0$.

The eddy viscosity and resistivity listed in Table I shows that λ^{bb*} and ν^{ub*} decrease as d increases. On the contrary, λ^{bu*} and ν^{uu*} first increases till $d = 4$ then decreases as d increases. Since MHD fluxes are proportional to these parameters, the corresponding fluxes decrease as d is increased beyond 4. Near $d = 2$, ν^{uu*} is negative, reminiscent of inverse cascade energy in two-dimensional fluid turbulence in the $5/3$ region. Also, λ^{bu*} is negative near $d = 2$, i.e., there is a negative energy cascade from b -sphere to outside u -sphere. The above results are consistent with the recent simulation results of Dar et al. [29] on two-dimensional MHD turbulence.

The variation of ν^{XY*} with r_A for $d = 3$ is displayed in Tables II. For large r_A , ν^{uu*} is close to the fluid turbulence ν^* . However, λ^{bb*} also finite. Hence there is a significant magnetic energy cascade from b -sphere to outside b -sphere even in fluid dominated case. As r_A is decreased, ν^{ub*} and λ^{bu*} increase, hence cascade rates from u -sphere to outside b -sphere and b -sphere to outside u -sphere start becoming important. Incidentally, both ν^{uu*} and λ^{bb*} decrease as r_A decreases.

In this section we have calculated the renormalized viscosity and resistivity for $\sigma_c = 0$. In the next section we will calculate these parameters for $\sigma_c \rightarrow 1$ limit.

III. RG CALCULATION: $\sigma_c \rightarrow 1$

The **u** and **b** correlation is very high when $\sigma_c \rightarrow 1$. For this case it is best to work with Elsässer variables $\mathbf{z}^\pm = \mathbf{u} \pm \mathbf{b}$. In terms of Elsässer variables, $\langle |z^+|^2 \rangle \gg \langle |z^-|^2 \rangle$. These types of fluctuations have been observed in the solar wind near the Sun. However, by the time the solar wind approaches Earth, the normalized cross helicity is close to zero.

In this section we will briefly discuss the RG treatment for the above case. For the following discussion we will denote $\langle |z^-|^2 \rangle / \langle |z^+|^2 \rangle = r = (1 - \sigma_c) / (1 + \sigma_c)$. Clearly $r \ll 1$.

MHD equation in terms of Elsässer variables are

$$(-i\omega + \nu_{(0)\pm\pm} k^2) z_i^\pm(\hat{k}) + \nu_{(0)\pm\mp} k^2 z_i^\mp(\hat{k}) = -i M_{ijm}(\mathbf{k}) \int d\hat{p} [z_j^\mp(\hat{p}) z_m^\pm(\hat{k} - \hat{p})] \quad (3.1)$$

where

$$M_{ijm}(\mathbf{k}) = k_j P_{im}(\mathbf{k}) \quad (3.2)$$

Note that the above equations contain four dissipative coefficients $\nu_{\pm\pm}$ and $\nu_{\pm\mp}$ instead of usual two constants $\nu_\pm = (\nu \pm \lambda)/2$. This is because $+-$ symmetry is broken in this case, and RG generates the other two constants. We carry out the same procedure as outlined in the previous section. After $n + 1$ steps of RG calculation, the above equations become

$$\begin{aligned} & [-i\omega \mp (\nu_{(n)\pm\pm}(k) + \delta\nu_{(n)\pm\pm}(k)) k^2] z_i^{\pm<}(\hat{k}) \\ & + (\nu_{(n)\pm\mp}(k) + \delta\nu_{(n)\pm\mp}(k)) k^2 z_i^{\mp<}(\hat{k}) = -i M_{ijm}(\mathbf{k}) \int d\hat{p} z_j^{\mp<}(\hat{p}) z_m^{\pm<}(\hat{k} - \hat{p}) \end{aligned} \quad (3.3)$$

with

$$\begin{aligned} \delta\nu_{(n)++}(k) = & \frac{1}{(d-1)k^2} \int_{\hat{p}+\hat{q}=\hat{k}}^\Delta d\hat{p} [S_1(k, p, q) G_{(n)}^{++}(\hat{p}) C^{--}(\hat{q}) + S_2(k, p, q) G_{(n)}^{+-}(\hat{p}) C^{--}(\hat{q}) \\ & + S_3(k, p, q) G_{(n)}^{-+}(\hat{p}) C^{+-}(\hat{q}) + S_4(k, p, q) G_{(n)}^{--}(\hat{p}) C^{+-}(\hat{q})] \end{aligned} \quad (3.4)$$

$$\begin{aligned} \delta\nu_{(n)+-}(k) = & \frac{1}{(d-1)k^2} \int_{\hat{p}+\hat{q}=\hat{k}}^\Delta d\hat{p} [S_1(k, p, q) G_{(n)}^{+-}(\hat{p}) C^{-+}(\hat{q}) + S_2(k, p, q) G_{(n)}^{++}(\hat{p}) C^{-+}(\hat{q}) \\ & + S_3(k, p, q) G_{(n)}^{--}(\hat{p}) C^{++}(\hat{q}) + S_4(k, p, q) G_{(n)}^{-+}(\hat{p}) C^{++}(\hat{q})] \end{aligned} \quad (3.5)$$

where the integral is performed over the $(n + 1)$ th shell (k_{n+1}, k_n) . The equations for the other two $\delta\nu$ s can be obtained by interchanging $+$ and $-$ signs. The inspection of Eqs. (3.4, 3.5) reveal that ν_{++} and ν_{-+} are of the order of r . Hence, we take the $\hat{\nu}$ matrix to be of the form

$$\hat{\nu}(k, \omega) = \begin{pmatrix} r\zeta & \alpha \\ r\psi & \beta \end{pmatrix} \quad (3.6)$$

The evaluation of Greens function and correlation function is quite involved, but it is in the same lines as followed in the previous section. The final expressions for the elements of $\delta\hat{\nu}$ are

$$\begin{aligned}\delta\zeta_{(n)}(k) = & \frac{1}{(d-1)k^2} \int^\Delta \frac{d\mathbf{p}}{(2\pi)^d} C^+(q) \{ S_1(k, p, q) \frac{1}{\beta_{(n)}(q)q^2} \\ & + S_2(k, p, q) \frac{\alpha_{(n)}(p)}{\beta_{(n)}(p)} \left(\frac{1}{\beta_{(n)}(p)p^2 + \beta_{(n)}(q)q^2} - \frac{1}{\beta_{(n)}(q)q^2} \right) \\ & - S_3(k, p, q) \frac{\alpha_{(n)}(q)}{\beta_{(n)}(q)} \left(\frac{1}{\beta_{(n)}(p)p^2 + \beta_{(n)}(q)q^2} - \frac{1}{\beta_{(n)}(p)p^2} \right) \}\end{aligned}\quad (3.7)$$

$$\delta\alpha_{(n)}(k) = \frac{1}{(d-1)k^2} \int^\Delta \frac{d\mathbf{p}}{(2\pi)^d} S_3(k, p, q) \frac{C^+(q)}{\beta_{(n)}(p)q^2} \quad (3.8)$$

$$\begin{aligned}\delta\psi_{(n)}(k) = & \frac{1}{(d-1)k^2} \int^\Delta \frac{d\mathbf{p}}{(2\pi)^d} C^+(q) \{ S_3(k, p, q) \frac{1}{\beta_{(n)}(q)q^2} \\ & + S_2(k, p, q) \frac{\alpha_{(n)}(q)}{\beta_{(n)}(q)} \left(\frac{1}{\beta_{(n)}(p)p^2 + \beta_{(n)}(q)q^2} - \frac{1}{\beta_{(n)}(p)p^2} \right) \\ & + S_4(k, p, q) \frac{\alpha_{(n)}(p)}{\beta_{(n)}(p)} \frac{1}{\beta_{(n)}(q)q^2} \}\end{aligned}\quad (3.9)$$

$$\delta\beta_{(n)}(k) = \frac{1}{(d-1)k^2} \int^\Delta \frac{d\mathbf{p}}{(2\pi)^d} S_1(k, p, q) \frac{C^+(q)}{\beta_{(n)}(p)p^2} \quad (3.10)$$

We substitute the following one-dimensional energy spectra in the above equations:

$$E^+(k) = K^+ \frac{(\Pi^+)^{4/3}}{(\Pi^-)^{2/3}} k^{-5/3} \quad (3.11)$$

$$E^-(k) = rE^+(k) \quad (3.12)$$

and the elements of $\hat{\nu}$ as

$$Z_{(n)}(k) = Z_{(n)}^* \sqrt{K^+} \frac{(\Pi^+)^{2/3}}{(\Pi^-)^{1/3}} k^{-4/3} \quad (3.13)$$

where Z stands for $\zeta, \alpha, \psi, \beta$. The renormalized Z^* 's are calculated using the procedure outlined in the previous section. For large n their values for $d = 3$ are

$$\hat{Z}^* = \begin{pmatrix} 0.60r & 0.10 \\ 11r & 0.59 \end{pmatrix} \quad (3.14)$$

and for $d = 2$ are

$$\hat{Z}^* = \begin{pmatrix} 0.95r & 0.54 \\ 1.10r & 0.54 \end{pmatrix} \quad (3.15)$$

Note that the solution converges for both $d = 2$ and $d = 3$.

The calculation of K^\pm and the fluxes are left for future studies (paper II).

IV. SUMMARY AND CONCLUSIONS

In this paper we have constructed a self-consistent RG scheme for MHD turbulence and showed that Kolmogorov-like energy spectrum is a consistent solution of MHD. In our RG scheme we assume that we are in the fully nonlinear range, and the renormalized energy spectrum is substituted for the correlation function. After the substitution of the correlation, the renormalized Greens function or renormalized viscosity and resistivity are computed iteratively. We find a Kolmogorov's powerlaw is a self-consistent solution of the RG equation for $d \geq d_c \approx 2.2$. This result is consistent with the recent theoretical [10,21,22], numerical [18–20], and observational studies of solar wind [16,17] that favor Kolmogorov's spectrum for MHD turbulence. Note that we do not carry out vertex renormalization; there is an implicit assumption that the vertex renormalization, if any, is included when we substitute renormalized energy spectrum (Kolmogorov's) in the RG equation.

For simplicity of the calculation we have taken two special cases: (1) $\sigma_c = 0$ and full range of r_A ; (2) $\sigma_c \rightarrow 1$ and $r_A = 1$. For these two cases, the renormalized viscosity and resistivity have been calculated for various space dimensions. For $\sigma_c = 0$, there exists a stable RG fix point for $d \geq d_c \approx 2.2$. The RG fixed point is unstable for $d < d_c$. Our result is consistent with that Liang and Diamond [9] where they conclude that the RG fixed point for $d = 2$ is unstable. Note however that the stability depends on the value of r_A and σ_c . An exhaustive study is required to ascertain the boundary of stability as a function of d , σ_c , and r_A .

There are some interesting trends as we vary space dimensionality. For $r_A = 1$, the parameters ν^{ub*} and λ^{bb*} decreases with the increase of d , but ν^{uu*} and λ^{bu*} first increase till $d \approx 4$ then decrease.

For $d = 3$, variation of r_A shows some interesting features. For large r_A , ν^* is close to the ν^* for pure fluid turbulence, but λ^* is also finite for this case. As r_A is decreased, ν^* increases and λ^* decreases. Another important result of our calculation is absence of turbulence for r_A near 0.25. In the $r_A \rightarrow 0$ (fully magnetic) limit, the MHD equations become linear, hence there is no turbulence. It was however surprising that turbulence disappear near $r_A = 0.25$ itself.

Our RG calculation for fluid turbulence ($r_A = \infty$) show several interesting features. The RG fixed point is stable for $d = 2$, and the renormalized viscosity is approximately -0.5 , a *negative* number. This is consistent with the inverse cascade of energy for $5/3$ region. Note however that for $d = 3$, the renormalized viscosity is 0.25, hence the energy cascade is forward consistent with Kolmogorov's hypothesis.

The values of renormalized viscosity and resistivity calculated by our calculation differs from that of Verma and Bhattacharjee [30], a calculation similar to Kraichnan's Direct-Interaction-Approximation calculation for fluid turbulence. In their calculation, they had assumed $\nu^{++} = \nu^{-+}$ and $\nu^{+-} = \nu^{--}$, which is correct only in a limited region of parameter space. In addition, they assumed a cutoff for the self-energy calculation to cure infrared divergence. We have overcome both these defects in the present calculation, and expect that the numbers reported here will match with the future simulation results. It is unfortunate that the RG scheme fails for $d = 2$. Therefore, several numerical results of 2D-MHD turbulence [18–20,29] could not be compared to the analytic results presented here.

Kraichnan's $3/2$ energy spectrum and $\Sigma^{uu} = \Sigma^{bb} \propto (kB_0)$ do not satisfy renormalization group equations [Eqs. (2.30–2.33)]. Hence $E(k) \propto k^{-3/2}$ is not a consistent solution of RG equations. This result is in agreement with the recent calculation by Verma [10] where it was shown that $B_0 = \text{constant}$ does not satisfy RG equations, but the renormalized mean magnetic field ($B_0 \propto k^{-1/3}$) and Kolmogorov's ($k^{-5/3}$) do satisfy the equations. From these arguments we can claim that Kraichnan's $3/2$ powerlaw is ruled out for strong MHD turbulence. However, $k^{-3/2}$ may still be considered in the frame work of weak turbulence theory.

In many of the earlier RG calculations [1,4] it is assumed that the dynamical system under consideration is forced by random noise at all scales. In those calculations, the noise and the vertex (coefficient of the nonlinear term) usually get renormalized along with the renormalization of dissipative coefficients. In contrast, in our scheme only the dissipative constants are renormalized, and the renormalization correction to other parameters (e.g. noise) are implicitly lumped into the full correlation function by assuming Kolmogorov's powerlaw. Our procedure is relatively simple, and one can easily calculate various interesting quantities. We hope that future developments in dynamical RG will be able to justify some of the assumptions made in our procedure.

To conclude, we have shown that Kolmogorov's spectrum is a consistent solution of MHD RG equation, and we have calculated the renormalized viscosity and resistivity. These results are in general agreement with the recent EDQNM and numerical results. Validation of the results presented here with numerical simulations will give us important insights into physics of MHD turbulence.

ACKNOWLEDGMENTS

The author thanks J. K. Bhattacharjee for valuable discussions and insights from the inception to the end of the problem. He also benefitted greatly from the numerous discussions he had with G. Dar and V. Eswaran on simulation results.

APPENDIX A: PERTURBATIVE CALCULATION OF MHD EQUATION

The MHD equations (2.4, 2.5) can be written as

$$\begin{pmatrix} u_i(\hat{k}) \\ b_i(\hat{k}) \end{pmatrix} = \begin{pmatrix} G^{uu}(\hat{k}) & G^{ub}(\hat{k}) \\ G^{bu}(\hat{k}) & G^{bb}(\hat{k}) \end{pmatrix} \begin{pmatrix} -\frac{i}{2} P_{ijm}^+(\mathbf{k}) \int d\hat{p} [u_j(\hat{p}) u_m(\hat{k} - \hat{p}) - b_j(\hat{p}) b_m(\hat{k} - \hat{p})] \\ -i P_{ijm}^-(\mathbf{k}) \int d\hat{p} [u_j(\hat{p}) b_m(\hat{k} - \hat{p})] \end{pmatrix} \quad (\text{A1})$$

where the Greens function G can be obtained from $G^{-1}(\vec{k})$

$$G^{-1}(k, \omega) = \begin{pmatrix} -i\omega - \Sigma^{uu} & \Sigma^{ub} \\ \Sigma^{bu} & -i\omega - \Sigma^{bb} \end{pmatrix}. \quad (\text{A2})$$

We solve the above equation perturbatively keeping the terms to the first order (nonvanishing). As usual, we represent the integrals by Feynmann diagrams. To the leading order, the quantities u_i and b_i are expanded as

$$u_i = \text{---} = \text{---} \circ G^{uu} \circ \text{---} - \text{---} \circ G^{uu} \circ \text{---} + \text{---} \circ G^{ub} \circ \text{---} + \dots \quad (\text{A3})$$

$$b_i = \overbrace{\dots}^{G^{bu}} - \overbrace{\dots}^{G^{ub}} + \overbrace{\dots}^{G^{bb}} + \dots \quad (A4)$$

The variables u and b are represented by solid and dashed line respectively. The quantity $G^{uu}, G^{ub}, G^{bb}, G^{bu}$ are represented by thick wiggly (photon), thin wiggly, thick curly (gluon), and thin curly lines respectively. The filled circle represents $(-i/2)P_{ijm}^+$ vertex, while the empty circle represents $-iP_{ijm}^-$ vertex.

The substitution of $u_i^>$ and $b_i^>$ in the second bracketed terms of (2.13, 2.14), denoted by $I_2^{u,b}$, will yield

$$I_2^u = \quad 2 \begin{array}{c} \bullet \\ \diagup \\ \diagdown \end{array} > - \quad 2 \begin{array}{c} \bullet \\ \diagup \\ \diagdown \end{array} < \quad (A5)$$

$$I_2^b = \text{Diagram 1} + \text{Diagram 2} \quad (A6)$$

We illustrate the expansion of one of the above diagrams:

In the above diagrams solid lines denote C^{uu} , and the dotted lines denote C^{ub} . The correlation function C^{bb} is denoted by dashed line. As mentioned earlier, the wiggly and curly lines denote various Green's functions. All the diagrams except 4,8,12, and 16th of the above equation can be shown to be trivially zero using Eqs. (2.15—2.21). We assume that 4,8,12, and 16th diagrams are also zero, as usually done in turbulence RG calculations [4,5]. Similarly we can show that all other diagrams of I_2^u and I_2^b are zero, hence, $I_2^u = I_2^b = 0$ to first order.

The third bracketed terms of (2.13, 2.14), denoted by I_3^u and I_3^b , are diagrammatically represented as

$$\begin{aligned}
I_3^u &= \text{Diagram 1} - \text{Diagram 2} \\
&= -\delta\Sigma^{uu}(k) \text{---} - \delta\Sigma^{ub}(k) \text{---} \text{---} \quad (A8)
\end{aligned}$$

$$\begin{aligned}
I_3^b &= \text{Diagram 3} \\
&= -\delta\Sigma^{bu}(k) \text{---} - \delta\Sigma^{bb}(k) \text{---} \text{---} \quad (A9)
\end{aligned}$$

where

$$-(d-1)\delta\Sigma^{uu} = \text{Diagram 4} - 2\text{Diagram 5} + 2\text{Diagram 6} - 4\text{Diagram 7} \quad (A10)$$

$$-(d-1)\delta\Sigma^{ub} = -4\text{Diagram 8} + 2\text{Diagram 9} + 4\text{Diagram 10} - 2\text{Diagram 11} \quad (A11)$$

$$-(d-1)\delta\Sigma^{bu} = 2\text{Diagram 12} + \text{Diagram 13} + \text{Diagram 14} - 2\text{Diagram 15} \quad (A12)$$

$$-(d-1)\delta\Sigma^{bb} = 2\text{Diagram 16} + \text{Diagram 17} + \text{Diagram 18} - \text{Diagram 19} \quad (A13)$$

In Eqs. (A10–A13) we have omitted all the vanishing diagrams (similar to those appearing in I_2). Looking at the all the terms, we observe I_3^u renormalizes Σ^{uu} and Σ^{ub} , while I_3^b renormalizes Σ^{bb} and Σ^{bu} . The algebraic expressions for the above diagrams are given by Eqs. (2.24–2.27).

APPENDIX B: VALUES OF S_i

$S_i(k, p, q)$ are formed by contracting tensors $P_{ijm}^+, P_{ijm}^-, P_{ij}$ and M_{ijm} (see Eqs. (2.8,2.10,3.2)). On simplification S_i s become functions of k, p, q and cosines x, y, z defined as

$$\mathbf{p} \cdot \mathbf{q} = -pqx; \quad \mathbf{q} \cdot \mathbf{k} = qky; \quad \mathbf{p} \cdot \mathbf{k} = pkz. \quad (B1)$$

The algebraic expressions for various $S_i(k, p, q)$ are given below.

$$\begin{aligned}
S_1(k, p, q) &= M_{bjm}(k)M_{mab}(p)P_{ja}(q) \\
&= kp(d-2+z^2)(z+xy) \quad (B2)
\end{aligned}$$

$$\begin{aligned}
S_2(k, p, q) &= M_{ajm}(k)M_{mab}(p)P_{jb}(q) \\
&= kp(-z+z^3+y^2z+xyz^2) \quad (B3)
\end{aligned}$$

$$\begin{aligned}
S_3(k, p, q) &= M_{bjm}(k)M_{jab}(p)P_{ma}(q) \\
&= kp(-z+z^3+x^2z+xyz^2) \quad (B4)
\end{aligned}$$

$$S_4(k, p, q) = M_{ajm}(k)M_{jab}(p)P_{mb}(q)$$

$$= kp(-z + z^3 + xy + x^2z + y^2x + xyz^2) \quad (B5)$$

$$\begin{aligned} S(k, p, q) &= P_{bjm}^+(k) P_{mab}^+(p) P_{ja}(q) \\ &= kp((d-3)z + 2z^3 + (d-1)xy) \end{aligned} \quad (B6)$$

$$\begin{aligned} S_5(k, p, q) &= P_{bjm}^+(k) P_{mab}^-(p) P_{ja}(q) \\ &= kp((d-1)z + (d-3)xy - 2y^2z) \end{aligned} \quad (B7)$$

$$\begin{aligned} S_6(k, p, q) &= P_{ajm}^+(k) P_{mba}^-(p) P_{jb}(q) \\ &= -S_5(k, p, q) \end{aligned} \quad (B8)$$

$$\begin{aligned} S_7(k, p, q) &= P_{ijm}^-(k) P_{mab}^+(p) P_{ja}(q) P_{ib}(k) \\ &= S_5(p, k, q) \end{aligned} \quad (B9)$$

$$\begin{aligned} S_8(k, p, q) &= P_{ijm}^-(k) P_{jab}^+(p) P_{ma}(q) P_{ib}(k) \\ &= -S_5(p, k, q) \end{aligned} \quad (B10)$$

$$\begin{aligned} S_9(k, p, q) &= P_{ijm}^-(k) P_{mab}^-(p) P_{ja}(q) P_{ib}(k) \\ &= kp(d-1)(z + xy) \end{aligned} \quad (B11)$$

$$\begin{aligned} S_{10}(k, p, q) &= P_{ijm}^-(k) P_{mab}^-(p) P_{jb}(q) P_{ia}(k) \\ &= -S_9(k, p, q) \end{aligned} \quad (B12)$$

$$\begin{aligned} S_{11}(k, p, q) &= P_{ijm}^-(k) P_{jab}^-(p) P_{ma}(q) P_{ib}(k) \\ &= -S_9(k, p, q) \end{aligned} \quad (B13)$$

$$\begin{aligned} S_{12}(k, p, q) &= P_{ijm}^-(k) P_{jab}^-(p) P_{mb}(q) P_{ia}(k) \\ &= S_9(k, p, q) \end{aligned} \quad (B14)$$

There are many useful relationships between $S_i(k, p, q)$. Some of them are

$$S(k, p, q) = S_1(k, p, q) + S_2(k, p, q) + S_3(k, p, q) + S_4(k, p, q) \quad (B15)$$

$$S_5(k, p, q) = S_1(k, p, q) - S_2(k, p, q) + S_3(k, p, q) - S_4(k, p, q) \quad (B16)$$

[1] D. Forster, D. R. Nelson, and M. J. Stephen, Phys. Rev. A **16**, 732 (1977).
[2] C. DeDominicis and P. C. Martin, Phys. Rev. A **19**, 419 (1979).
[3] J. D. Fournier and U. Frisch, Phys. Rev. A **17**, 747 (1979).
[4] V. Yakhot and S. A. Orszag, J. Sci. Comput. **1**, 3 (1986).
[5] W. D. McComb, *The Physics of Fluid Turbulence* (Clarendon, Oxford, 1990).
[6] W. D. McComb, Rep. Prog. Phys. **58**, 1117 (1995).
[7] J. D. Fournier, P.-L. Sulem, and A. Pouquet, J. Phys. A **15**, 1393 (1982).
[8] S. J. Camargo and H. Tasso, Phys. Fluids B **4**, 1199 (1992).
[9] W. Z. Liang and P. H. Diamond, Phys. Fluids B **5**, 63 (1993).
[10] M. K. Verma, Phys. Plasma **6**, 1455 (1999).
[11] R. H. Kraichnan, Phys. Fluids **8**, 1385 (1965).
[12] P. S. Iroshnikov, Sov. Astron. I. **7**, 566 (1964).
[13] E. Marsch, in *Reviews in Modern Astronomy*, edited by G. Klare (Springer-Verlag, Berlin, 1990), p. 43.
[14] W. H. Matthaeus and Y. Zhou, Phys. Fluids B **1**, 1929 (1989).
[15] Y. Zhou and W. H. Matthaeus, J. Geophys. Res. **95**, 10291 (1990).
[16] W. H. Matthaeus and M. L. Goldstein, J. Geophys. Res. **87**, 6011 (1982).
[17] E. Marsch and C.-Y. Tu, J. Geophys. Res. **95**, 8211 (1990).
[18] M. K. Verma *et al.*, J. Geophys. Res. **101**, 21619 (1996).
[19] W. C. Müller and D. Biskamp, Phys. Rev. Lett. **84**, 475 (2000).
[20] D. Biskamp and W. C. Müller, Phys. Plasma **7**, 4889 (2000).
[21] S. Sridhar and P. Goldreich, Astrophys. J. **432**, 612 (1994).
[22] P. Goldreich and S. Sridhar, Astrophys. J. **438**, 763 (1995).

[23] J. D. Fournier, U. Frisch, and A. Rose, J. Phys. A **11**, 187 (1978).
[24] W. D. McComb and A. G. Watt, Phys. Rev. A **46**, 4797 (1992).
[25] Y. Zhou and G. Vahala, Phys. Rev. E **47**, 2503 (1993).
[26] A. Pouquet, J. Fluid Mech. **88**, 1 (1994).
[27] A. Ishizawa and Y. Hattori, chao-dyn/9810036 (1998).
[28] A. Ishizawa and Y. Hattori, J. Phy. Soc. Jpn. **67**, 441 (1998).
[29] G. Dar, M. K. Verma, and V. Eswaran, **chao-dyn/9810032**, submitted to Physica D (2000).
[30] M. K. Verma and J. K. Bhattacharjee, Europhys. Lett. **31**, 195 (1995).

TABLE I. The values of ν^* , λ^* , ν^{uu*} , ν^{ub*} , λ^{bu*} , λ^{bb*} for various space dimensions d with $r_A = 1$ and $\sigma_c = 0$.

d	ν^*	λ^*	ν^{uu*}	ν^{ub*}	λ^{bu*}	λ^{bb*}
2.1	--	--	--	--	--	--
2.2	1.91	0.32	-0.041	1.96	-0.44	0.76
2.5	1.24	0.57	0.089	1.15	-0.15	0.72
3.0	1.00	0.69	0.20	0.80	0.078	0.61
4.0	0.83	0.70	0.27	0.56	0.21	0.49
7.0	0.62	0.59	0.26	0.36	0.25	0.34
10.0	0.51	0.50	0.23	0.28	0.22	0.28
50.0	0.23	0.23	0.11	0.12	0.11	0.12
100	0.135	0.135	0.065	0.069	0.066	0.069

TABLE II. The values of ν^* , λ^* , ν^{uu*} , ν^{ub*} , λ^{bu*} , λ^{bb*} for various r_A when **d = 3** and $\sigma_c = 0$.

r_A	ν^*	λ^*	ν^{uu*}	ν^{ub*}	λ^{bu*}	λ^{bb*}
∞	0.38	--	0.38	--	--	--
5000	0.36	0.85	0.36	1.4E-4	-0.023	0.87
100	0.36	0.85	0.36	7.3E-3	-0.022	0.87
5	0.47	0.82	0.32	0.15	-4.7E-4	0.82
2	0.65	0.78	0.27	0.38	0.031	0.75
1	1.00	0.69	0.20	0.80	0.078	0.61
0.5	2.11	0.50	0.11	2.00	0.15	0.35
0.3	11.0	0.14	0.022	11.0	0.082	0.053
0.2	--	--	--	--	--	--

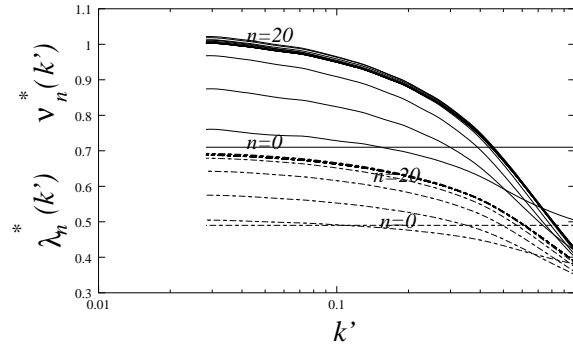


FIG. 1. Plot of $\nu^*(k')$ and $\lambda^*(k')$ vs. k' for $d = 3$ and $\sigma_c = 0, r_A = 1$. Values at various iterations are shown by different curves.

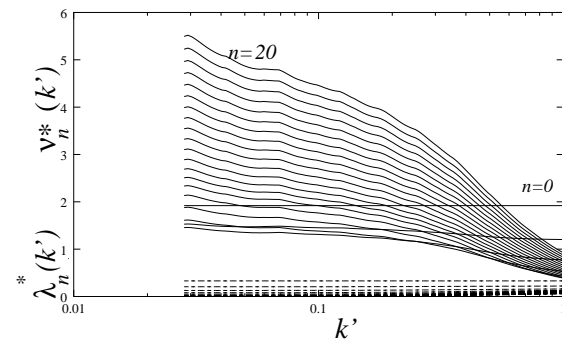


FIG. 2. Plot of $\nu^*(k')$ and $\lambda^*(k')$ vs. k' for $d = 2$ and $\sigma_c = 0, r_A = 1$.

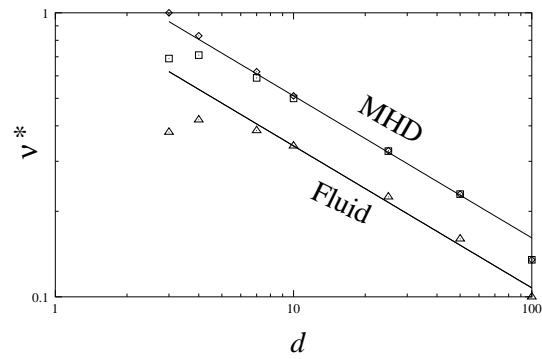


FIG. 3. Plot of asymptotic ν^* and λ^* vs. d for $\sigma_c = 0$ and $r_A = 1$. The fluid ν^* is also plotted for reference. The solid lines are the $d^{-1/2}$ curves.